

# PTEN knockdown with the Y444F mutant AAV2 vector promotes axonal regeneration in the adult optic nerve

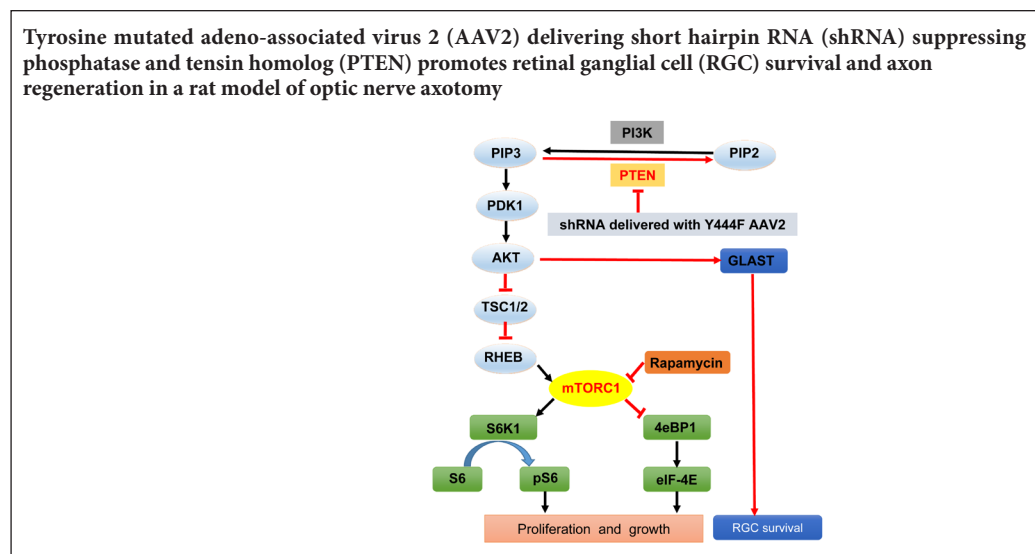
Zheng-ru Huang<sup>1,2</sup>, Hai-ying Chen<sup>2</sup>, Zi-zhong Hu<sup>1</sup>, Ping Xie<sup>1</sup>, Qing-huai Liu<sup>1,\*</sup>

1 Department of Ophthalmology, the First Affiliated Hospital of Nanjing Medical University, Nanjing, Jiangsu Province, China

2 Department of Ophthalmology, the Second People's Hospital of Changshu, Changshu, Jiangsu Province, China

**Funding:** This study was supported by the Research Foundation of Jiangsu Provincial Commission of Health and Family Planning of China, No. H201653, and the Research Foundation of Changshu Science and Technology Bureau of China, No. CS201616.

## Graphical Abstract



\*Correspondence to:  
Qing-huai Liu, Ph.D.,  
liuqh@njmu.edu.cn.

orcid:  
0000-0003-0351-136X  
(Qing-huai Liu)

doi: 10.4103/1673-5374.224381

Accepted: 2017-10-09

## Abstract

The lack of axonal regeneration is the major cause of vision loss after optic nerve injury in adult mammals. Activating the PI3K/AKT/mTOR signaling pathway has been shown to enhance the intrinsic growth capacity of neurons and to facilitate axonal regeneration in the central nervous system after injury. The deletion of the mTOR negative regulator phosphatase and tensin homolog (PTEN) enhances regeneration of adult corticospinal neurons and ganglion cells. In the present study, we used a tyrosine-mutated (Y444F) AAV2 vector to efficiently express a short hairpin RNA (shRNA) for silencing PTEN expression in retinal ganglion cells. We evaluated cell survival and axonal regeneration in a rat model of optic nerve axotomy. The rats received an intravitreal injection of wildtype AAV2 or Y444F mutant AAV2 (both carrying shRNA to PTEN) 4 weeks before optic nerve axotomy. Compared with the wildtype AAV2 vector, the Y444F mutant AAV2 vector enhanced retinal ganglia cell survival and stimulated axonal regeneration to a greater extent 6 weeks after axotomy. Moreover, post-axotomy injection of the Y444F AAV2 vector expressing the shRNA to PTEN rescued ~19% of retinal ganglion cells and induced axons to regenerate near to the optic chiasm. Taken together, our results demonstrate that PTEN knockdown with the Y444F AAV2 vector promotes retinal ganglion cell survival and stimulates long-distance axonal regeneration after optic nerve axotomy. Therefore, the Y444F AAV2 vector might be a promising gene therapy tool for treating optic nerve injury.

**Key Words:** nerve regeneration; optic nerve; axotomy; gene therapy; Müller cell; retinal ganglion cell; AAV2; shRNA; PTEN; GLAST; mTOR; neural regeneration

## Introduction

Apoptosis of retinal ganglion cells (RGCs) is the key feature of traumatic optic neuropathy (Moore and Goldberg, 2010; Yang and Yang, 2012). As a part of the central nervous system, the optic nerve in mammals has a very limited ability to regenerate its axons after injury, resulting in irreversible vision loss. The failure of axonal regeneration has been attributed to the apoptosis of RGCs, insufficient intrinsic growth capacity of mature neurons, lack of suitable stimuli, and an inhibitory ex-

tracellular environment (Moore and Goldberg, 2010; Fischer and Leibinger, 2012). Over the last few decades, numerous studies have shown that activation of the intrinsic growth capacity is able to induce a robust regenerative response in mature axotomized RGCs (Goldberg, 2004; Yang and Yang, 2012). Deletion of phosphatase and tensin homolog (PTEN), a negative regulator of mammalian target of rapamycin (mTOR), has been demonstrated to enhance the regeneration of adult corticospinal neurons and RGCs (Park et al., 2008; Liu et al.,

2010). However, conditional gene deletion cannot currently be translated to clinical practice, and therapies based on small-interfering RNA (siRNA) to knockdown the target gene may be potentially most useful for treatment of optic nerve diseases, such as glaucomatous optic neuropathy (Guzman-Aranguez et al., 2013).

Although adeno-associated virus 2 (AAV2) is currently the most efficient vector for transduction of adult RGCs by intravitreal injection (Hellström and Harvey, 2011; Tshilenge et al., 2016), it takes a long time (more than 2 weeks) after injection to reach therapeutic levels of gene expression in the retina to rescue RGCs in traumatic optic neuropathy, a disease characterized by quick retinal deterioration (Xie et al., 2002; Hellström et al., 2011). Fortunately, site-directed tyrosine (Y)-to-phenylalanine (F) mutation of capsid surface-exposed and highly conserved tyrosine residues has been reported to dramatically increase the transduction efficiency of self-complementary AAV2 following intraocular injection (Petrus-Silva et al., 2009; Miao et al., 2016). Therefore, we hypothesized that Y-to-F mutated AAV2 might have great potential role in gene therapy for traumatic optic neuropathy.

In the present study, we evaluated the intraocular transduction characteristics of intravitreally injected Y-to-F mutated AAV2. We then used this vector to deliver shRNA to suppress PTEN and activate the PI3K/AKT/mTOR signaling pathway to promote RGC survival and axonal regeneration.

## Materials and Methods

### Animals

A total of 155 specific-pathogen-free female Sprague-Dawley rats, weighing 200–250 g, 8 weeks of age, were purchased from SLRC Laboratory (Shanghai, China) (license No. SCXK 2012-002) and were used for all experiments. The rats were housed in Makrolon polycarbonate cages with a 12-hour light/dark cycle, and allowed free access to food and water. All surgeries, including intravitreal injection, optic nerve axotomy, and stereotactical injection, were performed under deep anesthesia with intraperitoneal injection of 3% pentobarbital (50 mg/kg body weight). Animals were treated in compliance with the Association for Research in Vision and Ophthalmology Statement for the Use of Animals in Ophthalmic and Vision Research, and study protocols were approved by the Institutional Animal Care and Use Committee of Nanjing Medical University (approval No. 2015-0076).

### Construction of tyrosine-mutated AAV2 capsid plasmids

Single (Y444F), quadruple (Y272, 444, 500, 730F) and sextuple (Y252, 272, 444, 500, 704, 730) mutagenesis of surface-exposed tyrosine residues on AAV2 VP3 was generated with a two-stage procedure using QuikChange II site-directed mutagenesis of the pAAV-RC plasmid, as previously described (Zhong et al., 2008b). Briefly, in stage one, two polymerase chain reaction (PCR) extension reactions were performed in separate tubes for each mutant. One tube contained the forward PCR primer and the other contained the reverse primer. In stage two, the two reactions were mixed and a standard PCR mutagenesis procedure was carried out. PCR primers were designed to introduce changes from tyrosine to phenylalanine residues and a silent change to create a new restriction

endonuclease site for screening purposes.

### Production of pAAV-shRNA.PTEN-GFP plasmid

The most effective shRNA targeting PTEN was selected based on a previous report (Lewandowski and Steward, 2014). The sequence of this shRNA was cloned into the pAAV-U6-CAG-ZsGreen vector, as described previously (Koch et al., 2011a) (Figure 1). In brief, 1  $\mu$ L of the forward primer and 1  $\mu$ L of the reverse primer containing the shRNA sequence were dissolved in 16  $\mu$ L water and 2  $\mu$ L of 10 $\times$  annealing buffer (100 mM Tris, pH 7.5, 1 M NaCl and 10 mM ethylenediamine tetraacetic acid). The solution was boiled for 5 minutes and then cooled to room temperature. Annealed oligos were ligated to a *Bam*H I/*Eco*R I-cut backbone fragment of pAAV-U6-CAG-ZsGreen. The sequences of the shRNA primers were as follows (in bold: sequence of siRNA-sense and siRNA-antisense strands; in italics: sequences of the hairpin turns). shRNA.PTEN forward primer: 5'-GA TCC **GGC ACT GTT GTT TCA CAA GAT TTC AAG AGA ATC TTG TGA AAC AAC AGT GCC TTT TTT C-3'**; shRNA.PTEN reverse primer: 5'-AA TTG AAA **AAA GGC ACT GTT GTT TCA CAA GAT TCT CTT GAA AAC TTG TGA AAC AAC AGT GCC G-3'**. The plasmid was sequenced to confirm identity.

### Production of AAV2 vectors

Production of AAV2-GFP (wildtype (Wt), single mutant, quadruple mutant, and sextuple mutant), Wt AAV2-shRNA.PTEN-GFP and Y444F AAV2-shRNA.PTEN-GFP were performed as reported before (Zolotukhin et al., 1999). Briefly, HEK293 cells were transfected with calcium phosphate, HEPES-buffered saline and a serotype-specific plasmid complex containing 10  $\mu$ g pAAV-RC/mutated pAAV-RC, 20  $\mu$ g pHelper (Stratagene, La Jolla, CA, USA) and 10  $\mu$ g pAAV-GFP or pAAV-shRNA.PTEN-GFP plasmid. Then, 72 hours after transfection, cells were harvested and AAV were purified by dialysis and virus gradient centrifugation in iodixanol. Protein liquid chromatography was performed to obtain high-titer viral stocks. The viral titers were determined using quantitative

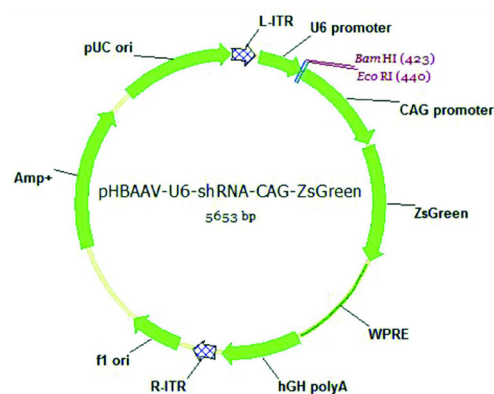


**Figure 1** Map of the AAV2 construct used to knockdown PTEN. shRNA.PTEN was inserted between the *Bam*H I and *Eco*R I sites, and expressed under the control of an U6 promoter. A robust and non-cell-specific CAG promoter controlled the expression of ZsGreen, acting as a reporter. R-LTR: Right long terminal repeat; L-LTR: left long terminal repeat; WPRE: woodchuck hepatitis virus post-transcriptional regulatory element; CAG: chicken beta actin; AAV2: adeno-associated virus 2; PTEN: phosphatase and tensin homolog.

PCR and normalized to  $1.0 \times 10^{12}$  viral genomes per milliliter (vg/mL) using balanced salt solution.

#### Transfection via intravitreal injection

AAV2 vectors (5  $\mu$ L, titers at  $1.0 \times 10^{12}$ ) or cholera toxin  $\beta$  subunit-conjugated fluorescein isothiocyanate C (CTB-FITC) (5  $\mu$ L of 0.2%; Sigma, St. Louis, MO, USA) were intravitreally injected using a 5- $\mu$ L Hamilton syringe (Hamilton, Bonaduz, Switzerland) (Koch et al., 2014). Briefly, the needle was inserted into the peripheral retina, just behind the ora serrata, and was carefully positioned to avoid damage. Rats with traumatic cataract, retinal detachment, or vitreous hemorrhage were excluded from this study.

#### Establishment of the optic nerve axotomy model

Optic nerve axotomy of the right eye was performed as reported previously (Koch et al., 2011b; Cen et al., 2017). In brief, the lateral canthus was incised along the orbital rim and the lacrimal gland was moved to the side. The eyeball was slightly rotated by pulling the superior rectus muscle. The optic nerve was then exposed intraorbitally, and crushed with jeweler's forceps (Dumont #5; Roboz, Switzerland) at a distance of at least 2 mm behind the eyeball for approximately 10 seconds, avoiding damage to the ophthalmic artery. The vascular integrity of the retina was examined by fundoscopy. Rats in which the retinal vessel was injured were excluded from the study.

#### Immunofluorescence

Rats were given a lethal overdose of anesthesia and transcardially perfused with 4% paraformaldehyde. Eyes were post-fixed in the same fixative, cryoprotected in 30% sucrose overnight at 4°C, and frozen in optimal cutting temperature compound. For immunostaining of phospho-S6 ribosomal protein (pS6) and glutamine synthetase, longitudinal frozen sections of the eyes were cut at 8  $\mu$ m thickness. For quantifying the density of RGCs, whole retinas were dissected out. Frozen sections were blocked with immunostaining blocking buffer (Beyotime, Shanghai, China) and permeabilized with 0.2% Triton X-100 for 1 hour at room temperature. Subsequently, the sections were incubated overnight at 4°C with rabbit anti-rat pS6 monoclonal antibody (1:100; Cell Signaling Technology, Danvers, MA, USA), and rabbit anti-rat glutamine synthetase monoclonal antibody (1:250; Abcam, Cambridge, MA, USA). Retinas were blocked with immunostaining blocking buffer and permeabilized with 0.2% Triton X-100 for 2 hours at room temperature. The retinas were immunostained overnight at 4°C with rabbit anti-rat neuronal class III  $\beta$ -tubulin (TUJ1) monoclonal antibody (1:250; Beyotime, Shanghai, China), which specifically labels adult RGCs (Park et al., 2008). The sections or retinas were rinsed with 0.1 M phosphate-buffered saline for 5 minutes and incubated with goat anti-rabbit secondary antibody conjugated to Cy3 (1:500; Beyotime) for 1 hour at room temperature. After washing, the sections were examined under a fluorescence microscope (Nikon Eclipse50i, Tokyo, Japan), and images were captured with a CCD camera. GFP staining intensity in flat mounts was quantified from fluorescence microscopic images using ImageJ software (National Institutes of Health, Bethesda, MD, USA) to determine the mean fluorescence intensity in pixels per image. The retinas immunostained with TUJ1 antibody

were mounted onto pre-coated glass slides, and the images were captured under the fluorescence microscope. Sixteen fields in the mid portion of the retina (approximately 0.276 mm<sup>2</sup> per field at 100 $\times$  magnification), radially distributed at 1 mm to 2 mm from the optic nerve disc, were sampled per retina. The total TUJ1-positive cells in each image were counted, and the density of RGCs was calculated.

#### Western blot assay

Total retinal protein was extracted and quantified using a bicinchoninic acid protein assay kit (Beyotime). Protein samples (30  $\mu$ g) were separated on 10% SDS-PAGE gels and transferred to polyvinylidene fluoride membranes (0.22- $\mu$ m; Millipore, Billerica, MA, USA). Membranes were incubated with a rabbit anti-rat glutamate aspartate transporter (GLAST) monoclonal antibody (1:2,500; Abcam), rabbit anti-rat pS6 monoclonal antibody (1:2,000; Cell Signaling Technology) or rabbit anti-rat glyceraldehyde-3-phosphate dehydrogenase (GAPDH) monoclonal antibody (1:5,000; Beyotime) overnight at 4°C. After washing in Tris-buffered saline with Tween, the membranes were incubated with goat anti-rabbit horseradish peroxidase-conjugated secondary antibody (1:1,000; Beyotime) for 1 hour at room temperature. The immune complexes were detected by enhanced chemiluminescence (Millipore). The optical density of the bands was quantified by densitometry and normalized to GAPDH using ImageLab software (BioRad laboratories, Hercules, CA, USA). Each experiment was performed at least three times.

#### Assessment of regenerating axons

To visualize and quantify regenerating RGC axons, 5  $\mu$ L of 0.2% CTB-FITC was injected into the vitreous body for anterograde labeling using a Hamilton syringe 5 days before sacrifice. The orbital optic nerve segments, the optic chiasm and the brain were dissected out, post-fixed in 4% paraformaldehyde, and transferred to 30% sucrose solution overnight at 4°C, separately. Longitudinal frozen sections of optic nerves and coronal frozen sections of the optic chiasm and brain were cut at 8  $\mu$ m, 10  $\mu$ m and 14  $\mu$ m thickness, respectively, and thaw-mounted onto pre-coated glass slides. At least five non-consecutive sections were examined under the fluorescence microscope for each animal. The fluorescence intensities of the CTB-FITC signals in the optic nerve at different distances from the site of optic nerve axotomy were analyzed with ImageJ software (NIH, Bethesda, MD, USA).

#### Statistical analysis

All data are displayed as the mean  $\pm$  SD. Statistical analysis was carried out using Stata 11.4 software (StataCorp, College Station, TX, USA). One-way analysis of variance followed by the Bonferroni's *post hoc* test was used to compare multiple groups. Pairwise comparison between groups was performed using Student's *t*-test. A value of  $P < 0.05$  was considered statistically significant.

## Results

#### Efficiency of transgene expression of AAV2 vectors

To evaluate the efficiency of transgene expression, Wt AAV2, single mutant, quadruple mutant and sextuple mutant vectors

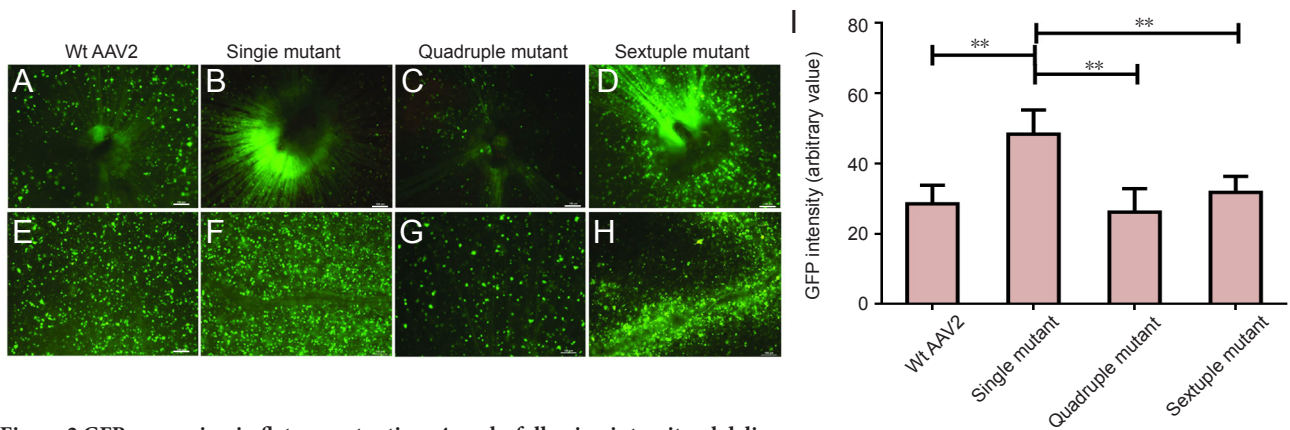


**Figure 2** GFP expression in flat-mount retinas 4 weeks following intravitreal delivery.

(A–H) GFP expression following transduction with wildtype (Wt) (A, E), single mutant (Y444F) (B, F), quadruple mutant (Y272, 444, 500, 730F) (C, G) and sextuple mutant (Y252, 272, 444, 500, 704, 730) (D, H) AAV2 vectors. (A–D) Images of the posterior retina including the optic disc; (E–H) images of the peripheral retina. (I) The GFP signal intensity for the single mutant was higher than for all other vectors. All pictures were taken with the same exposure time to evaluate GFP intensity using ImageJ software. Data are expressed as the mean  $\pm$  SD.  $**P < 0.01$  (analysis of variance followed by Bonferroni's *post hoc* test). Scale bars: 100  $\mu$ m. GFP: Green fluorescent protein.

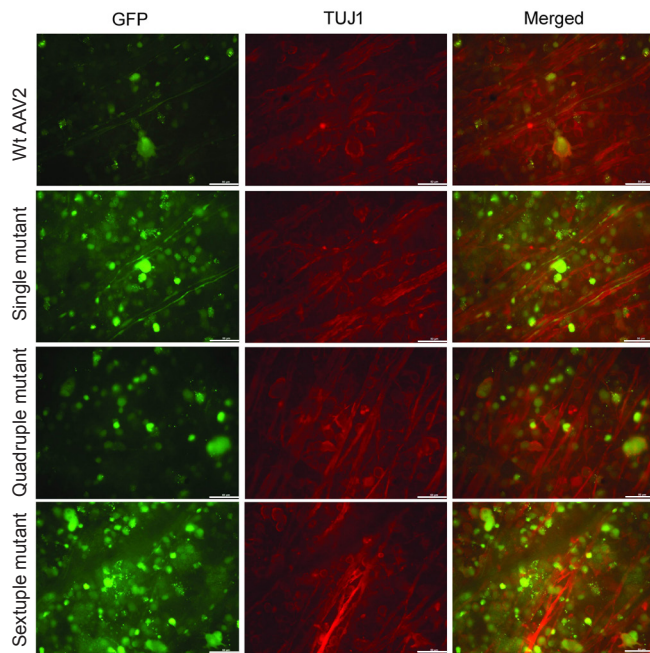


**Figure 3** Immunofluorescence in flat-mount whole retinas showing RGCs expressing the GFP transgene 4 weeks after intravitreal injection.

Merged image shows the colocalization of GFP and neuronal class III  $\beta$ -tubulin (TUJ1) in retinal flat-mounts from eyes injected with Wt AAV2, single mutant (Y444F), quadruple mutant (Y272, 444, 500, 730F) or sextuple mutant vectors, indicating that RGCs are transduced by the various AAV2 vectors. Scale bars: 100  $\mu$ m. GFP: Green fluorescent protein; RGCs: retinal ganglion cells; AAV2: adeno-associated virus 2.

were injected into the intact eyes of rats containing normal populations of RGCs. The fluorescence intensity of GFP expression in the eyes injected intravitreally with the various vectors was initially analyzed on retinal flat mounts to quantitatively evaluate the transduction capacity for each vector 4 weeks after injection. At this time point, Wt AAV2 and the quadruple mutant showed widespread GFP fluorescence, of moderate intensity, while the sextuple mutant displayed strong GFP fluorescence

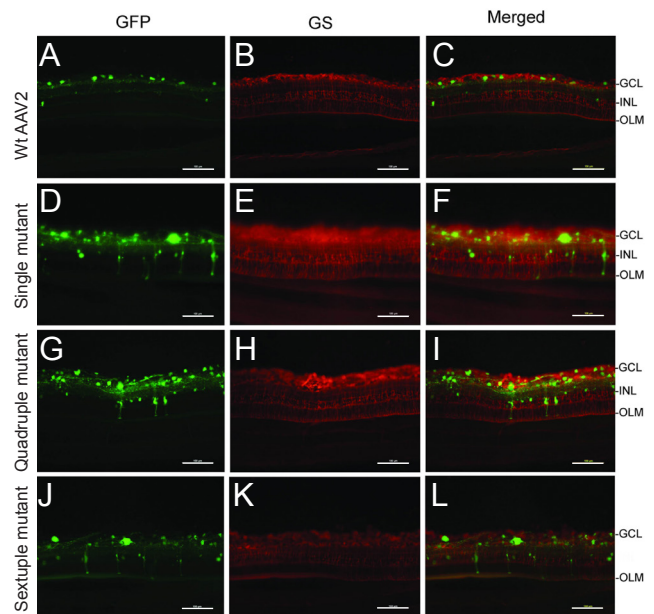


**Figure 4** Colocalization of GFP with the Müller cell marker GS in immunolabeled frozen retinal sections 4 weeks after intravitreal injection.

Infection with wildtype (Wt) (A–C) AAV2 resulted in GFP expression (green) in the GCL and occasionally in the INL. (D–L) Mutants produced a similar pattern of GFP expression in the GCL and INL. The majority of cells expressing GFP in the INL spanned nearly the full thickness of the retina, from the GCL to the OLM, which is characteristic of Müller glia (Newman and Reichenbach, 1996), and co-expressed GS. Scale bars: 100  $\mu$ m. GFP: Green fluorescent protein; GS: glutamine synthetase; GCL: ganglion cell layer; INL: inner nuclear layer; OLM: outer limiting membrane.

only in patchy areas around the blood vessels of the retina ( $n = 6$ ; **Figure 2A–H**). In contrast, the single mutant showed a significantly higher intensity of widespread GFP fluorescence compared to its wildtype counterpart or other mutants ( $n = 6$ ; **Figure 2I**). These results demonstrate that the Y444F AAV2 mutant displays significantly increased transduction efficiency relative to Wt AAV2.

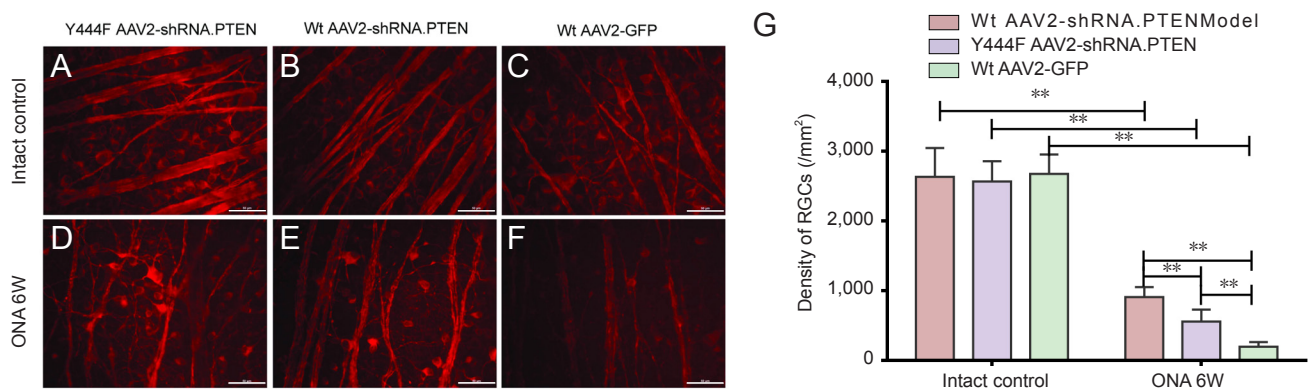


**Figure 5** Neuronal class III  $\beta$ -tubulin (TUJ1) immunolabeling for evaluating RGC survival 6 weeks after optic nerve axotomy in rats intravitreally injected with vector 4 weeks before lesioning.

(A–F) RGCs were visualized by immunolabeling with TUJ1 antibody to assess survival. Scale bars: 50  $\mu$ m. (G) The number of surviving RGCs was decreased significantly 6 weeks after axotomy. Compared with Wt AAV2-GFP, both Y444F AAV2-shRNA.PTEN and Wt AAV2-shRNA.PTEN significantly enhanced RGC survival, while Y444F AAV2-shRNA.PTEN further enhanced the survival of RGCs in comparison to Wt AAV2-shRNA.PTEN. Data are expressed as the mean  $\pm$  SD. \*\* $P < 0.01$  (analysis of variance followed by Bonferroni's *post hoc* test and Student's *t*-test). ONC: Optic nerve crush; RGCs: retinal ganglion cells; AAV2: adeno-associated virus 2; PTEN: phosphatase and tensin homolog; shRNA: short hairpin RNA.

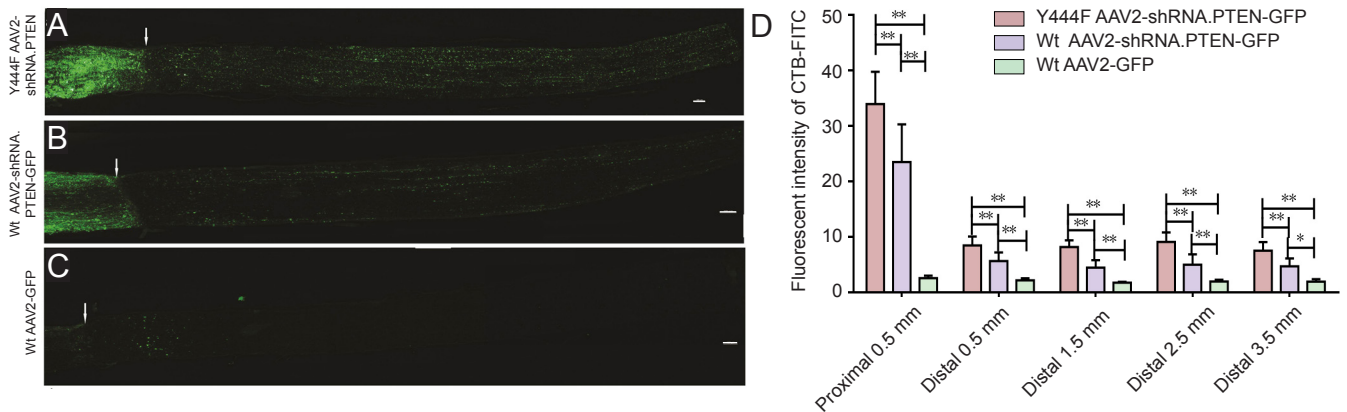


**Figure 6** Fluorescence images of longitudinal sections of the optic nerve showing axonal regeneration 6 weeks after optic nerve axotomy in rats intravitreally injected with vector 4 weeks before lesioning.

(A–C) CTB-FITC-labeled regenerating fibers in rats infected with Y444F AAV2-shRNA.PTEN (A), Wt AAV2-shRNA.PTEN (B) or Wt AAV2-GFP (C). Scale bars: 100  $\mu$ m. Arrows: optic nerve axotomy site. (D) Quantification of the fluorescence intensity at different distances to the lesion site. Transduction with Y444F AAV2-shRNA.PTEN or Wt AAV2-shRNA.PTEN increased the signal intensity at almost all analyzed positions, compared with Wt AAV2-GFP. Furthermore, Y444F AAV2-shRNA.PTEN produced higher signals compared with Wt AAV2-shRNA.PTEN. Transduction with Y444F AAV2-shRNA.PTEN or Wt AAV2-shRNA.PTEN resulted in a significant increase in the fluorescence intensity 500  $\mu$ m proximal to the optic nerve axotomy site compared with Wt AAV2-GFP. All pictures were taken with the same exposure time to evaluate GFP intensity using ImageJ software. Data are expressed as the mean  $\pm$  SD. \* $P < 0.05$ , \*\* $P < 0.01$  (analysis of variance followed by Bonferroni's *post hoc* test). CTB-FITC: Cholera toxin  $\beta$  subunit-conjugated fluorescein isothiocyanate; GFP: green fluorescent protein; AAV2: adeno-associated virus 2; PTEN: phosphatase and tensin homolog; shRNA: short hairpin RNA.

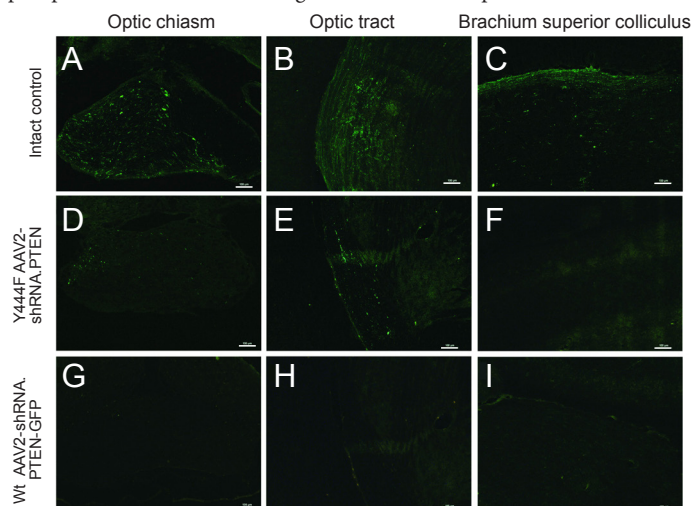


**Figure 7** CTB-FITC labeling for regenerating axons in the brain 6 weeks after optic nerve axotomy in rats intravitreally injected with vector 4 weeks before lesioning.

(A–C) CTB-FITC labeling showing nerve fibers in the optic chiasm, optic tract and brachium superior colliculus in normal control rats. (D, E) CTB-FITC labeling showing regenerating nerve fibers in the optic chiasm and optic tract of Y444F AAV2-shRNA.PTEN-injected rats. (F) No CTB-FITC-labeled nerve fibers were detected in the brachium superior colliculus. (G–I) No CTB-FITC-labeled nerve fibers were found in the optic chiasm, optic tract or brachium superior colliculus of Wt AAV2-shRNA.PTEN-injected rats. Scale bars: 100  $\mu$ m. CTB-FITC: Cholera toxin  $\beta$  subunit conjugated to fluorescein isothiocyanate; AAV2: adeno-associated virus 2; PTEN: phosphatase and tensin homolog; shRNA: short hairpin RNA.

### Assessment of AAV2 transgene expression

To evaluate the transduction properties of vectors 4 weeks after intravitreal injection, immunohistochemistry was performed on retinal flat mounts and frozen sections. In flat mounts, cells expressing GFP were stained with TUJ1 antibody ( $n = 6$ ; **Figure 3**). In frozen sections, all mutants displayed a similar pattern of GFP expression in the RGCs, Müller cells and other inner nuclear layer cells, while Wt AAV2 showed GFP expression in RGCs, and occasionally in inner nuclear layer cells ( $n = 6$ ; **Figure 4**). These results suggest that Wt AAV2 and the various mutants can transduce RGCs. Notably, compared with the Wt AAV2 vector, the Y-to-F mutant AAV2 vectors efficiently transduced both RGCs and Müller cells.

### RGC survival and axonal regeneration in rats administered AAV2 vectors before optic nerve axotomy

To evaluate their potential neuroprotective effects in RGCs, Y444F AAV2-shRNA.PTEN, Wt AAV2-shRNA.PTEN and Wt AAV2-GFP vectors were intravitreally injected 4 weeks before optic nerve axotomy. RGCs were identified by immunolabeling with TUJ1 antibody 6 weeks after optic nerve axotomy. The density of immunolabeled RGCs in the central region of the retina was quantified on flat mounts ( $n = 5$ ; **Figure 5A–F**). Substantial RGC loss was evident 6 weeks after optic nerve axotomy. The number of viable RGCs in retinas transduced with Wt AAV2-shRNA.PTEN ( $561 \pm 170/100\times$  field) was significantly higher compared with retinas transduced with Wt AAV2-GFP ( $201 \pm 65/100\times$  field) 6 weeks post-axotomy, and the survival of RGCs was further improved by transduction with Y444F AAV2-shRNA.PTEN ( $912 \pm 144/100\times$  field) ( $n = 5$ ; **Figure 5G**). In addition, the collapse of retinal nerve fibers in retinas transduced with Wt AAV2-shRNA.PTEN or Y444F AAV2-shRNA.PTEN was of reduced severity compared with retinas transduced with Wt AAV2-GFP ( $n = 5$ ; **Figure 5D–F**).

In addition to evaluating the survival of RGCs, we also assessed axonal regeneration. In rats transduced with Wt AAV2-GFP vector, only a few regenerating neurites were observed crossing the lesion site, and no neurite was observed greater than 500  $\mu\text{m}$  distal to the site of optic nerve axotomy ( $n = 5$ ; **Figure 6A**). In contrast, transduction with Y444F AAV2-shRNA.PTEN resulted in neurites regenerating over a long distance, extending from the lesion site towards the optic chiasm. Wt AAV2-shRNA.PTEN did not promote axonal regeneration towards the optic chiasm ( $n = 5$ ; **Figures 6B, 6C, 7D, 7G**). Quantification of the fluorescence intensities of CTB-FITC at all analyzed distances showed a significant increase in the Y444F AAV2-shRNA.PTEN group compared with the Wt AAV2-shRNA.PTEN or Wt AAV2-GFP group ( $n = 5$ ; **Figure 6D**). Notably, Y444F AAV2-shRNA.PTEN induced axonal regeneration as far as the optic tract ( $n = 5$ ; **Figure 7E, F, H, I**).

### Retinal expression of pS6 and GLAST in rats administered AAV2 vectors before optic nerve axotomy

To investigate the mechanisms underlying the effects of AAV2-mediated PTEN suppression on RGC survival and axonal regeneration, we assessed the expression of pS6 4 weeks after intravitreal injection. PTEN inhibition activates mTOR. The most widely used biochemical marker of mTOR activity is pS6,

a substrate of mTOR complex-1 (Park et al., 2008). Therefore, we evaluated the expression of pS6 by western blot assay and immunohistochemistry. Western blot assay showed that Y444F AAV2-shRNA.PTEN significantly increased pS6 expression in retinas compared with Wt AAV2-shRNA.PTEN or Wt AAV2-GFP 4 weeks after injection ( $P < 0.01$ ,  $P < 0.05$ ;  $n = 5$ ; **Figure 8A**). At 6 weeks after optic nerve axotomy, the expression of pS6 was significantly decreased in Wt AAV2-GFP-transduced retinas compared with intact retinas, and the expression of pS6 was significantly higher in Y444F AAV2-shRNA.PTEN and Wt AAV2-shRNA.PTEN-transduced retinas than in intact or Wt AAV2-GFP-transduced retinas ( $P < 0.01$ ,  $n = 5$ ; **Figure 8C**). At 4 weeks after injection, analysis of the percentage of pS6-positive cells in the ganglion cell layer revealed significant differences among Wt AAV2-GFP ( $7.08 \pm 2.57\%$ ), Wt AAV2-shRNA.PTEN ( $17.25 \pm 4.26\%$ ) and Y444F AAV2-shRNA.PTEN ( $23.25 \pm 4.31\%$ )-transduced retinas ( $n = 6$ ; **Figure 9**). Additionally, pS6-positive cells were also present in the inner nuclear layer of Y444F AAV2-shRNA.PTEN-transduced retinas, but were nearly completely absent in Wt AAV2-shRNA.PTEN and Wt AAV2-GFP-transduced retinas ( $n = 6$ ; **Figure 9**).

Next, we examined GLAST expression in retinas. GLAST expression was not significantly different among the various groups 4 weeks after virus injection (pre-axotomy) ( $P > 0.05$ ,  $n = 5$ ; **Figure 8B**). We then examined retinal GLAST expression 6 weeks after axotomy. A dramatic decrease in GLAST expression was found in the Y444F AAV2-shRNA.PTEN, Wt AAV2-shRNA.PTEN and Wt AAV2-GFP groups compared with the intact control group ( $P < 0.01$ ), but GLAST expression was higher in the Y444F AAV2-shRNA.PTEN group compared with the Wt AAV2-shRNA.PTEN or Wt AAV2-GFP group ( $P < 0.05$ ,  $n = 5$ ; **Figure 8D**).

### RGC survival and axonal regeneration after post-axotomy AAV2 injection

To mimic potential clinical situations, rats were intravitreally injected with Y444F AAV2-shRNA.PTEN immediately after optic nerve axotomy. Six weeks later, the density of RGCs was quantified and regenerating axons were examined. Although the number of surviving RGCs and the CTB-FITC fluorescence intensity of regenerating axons were significantly lower in post-axotomy-injected rats than in pre-axotomy-injected rats ( $n = 5$ ; **Figure 10A, B, D**), regenerating axons were observed to cross the lesion site and extend over long distances in the optic nerve ( $n = 5$ ; **Figure 10C**). Furthermore, regenerating fibers were observed in one of five optic chiasmata and no FITC-labeled fibers were visible in the optic tract ( $n = 5$ ; **Figure 10E**).

## Discussion

In this study, we investigated the effects of PTEN silencing by tyrosine-mutated AAV2 on axonal regeneration in the adult rat optic nerve. We found a much higher transduction efficiency of Y444F AAV2 for RGCs as well as Müller cells. Furthermore, when injected intravitreally before or immediately after optic nerve axotomy, this vector, carrying an shRNA to silence PTEN expression, promoted RGC survival and induced long-distance axonal regeneration by activating the PI3K/AKT/mTOR pathway and regulating glutamate homeostasis in rats.

Y444F AAV2 was the most efficient among the vectors tested, and this mutant had significantly higher transduction efficiency for RGCs and Müller cells. It has been shown that AAV2 strongly depends on heparan sulfate proteoglycans for transduction (Zaiss et al., 2015; Woodard et al., 2016). Heparan sulfate proteoglycans on the inner membrane may function as receptors, binding AAV2 and facilitating uptake by adult RGCs and Müller cells (Hellstrom et al., 2009; Petrs-Silva et al., 2009; Boye et al., 2016). The present results are consistent with previous studies showing that RGCs can be infected by intravitreally-injected Wt AAV2, while Müller cells can be occasionally transduced (Auricchio et al., 2001; Liang et al., 2003; Harvey et al., 2006). Once in the retina, AAV2 needs to overcome additional barriers to achieve efficient transduction. The ubiquitin-proteasome pathway is a major obstacle to AAV-mediated gene expression. This pathway degrades the viral particles during their intracellular trafficking from the cytoplasm to the nucleus, and involves the phosphorylation of tyrosine residues by the epidermal growth factor receptor (Ding et al., 2006; Zhong et al., 2008a). Thus, substitution of certain surface-exposed tyrosine residues on AAV2 capsids may allow the vectors to escape ubiquitination and proteasomal degradation. Interestingly, mutation of surface-exposed tyrosine residues on the AAV2 capsid can also lead to more efficient transduction of RGCs (Zhong et al., 2008b; Petrs-Silva et al., 2009), but not Müller cells (Petrs-Silva et al., 2011). AAV2 is the only serotype able to transduce RGCs efficiently, making it the only effective vector for therapies targeting glaucomatous optic neuropathy (Harvey et al., 2006). RGC apoptosis is the common result of glaucomatous optic neuropathy and traumatic optic neuropathy, although the underlying mechanisms may be different. Moreover, the progression of glaucomatous optic neuropathy is slow, while that of traumatic optic neuropathy is relatively rapid. The more potent transduction efficiency of Y444F AAV2 makes it a suitable gene delivery vector for treating traumatic optic neuropathy.

To our knowledge, we are the first to use Y444F AAV2 as a vector to deliver an shRNA targeting PTEN to promote RGC survival and activate its intrinsic axonal regenerative capacity. Deletion of PTEN, which is a negative regulator of mTOR, has been demonstrated to enhance the regeneration of adult corticospinal neurons and RGCs (Liu et al., 2010; Benowitz et al., 2017). However, conditional gene deletion prior to optic nerve injury is impossible to translate to clinical practice, while therapies based on RNA interference to knockdown a target gene may be most useful for treatment of optic nerve damage (Guzman-Arangué et al., 2013).

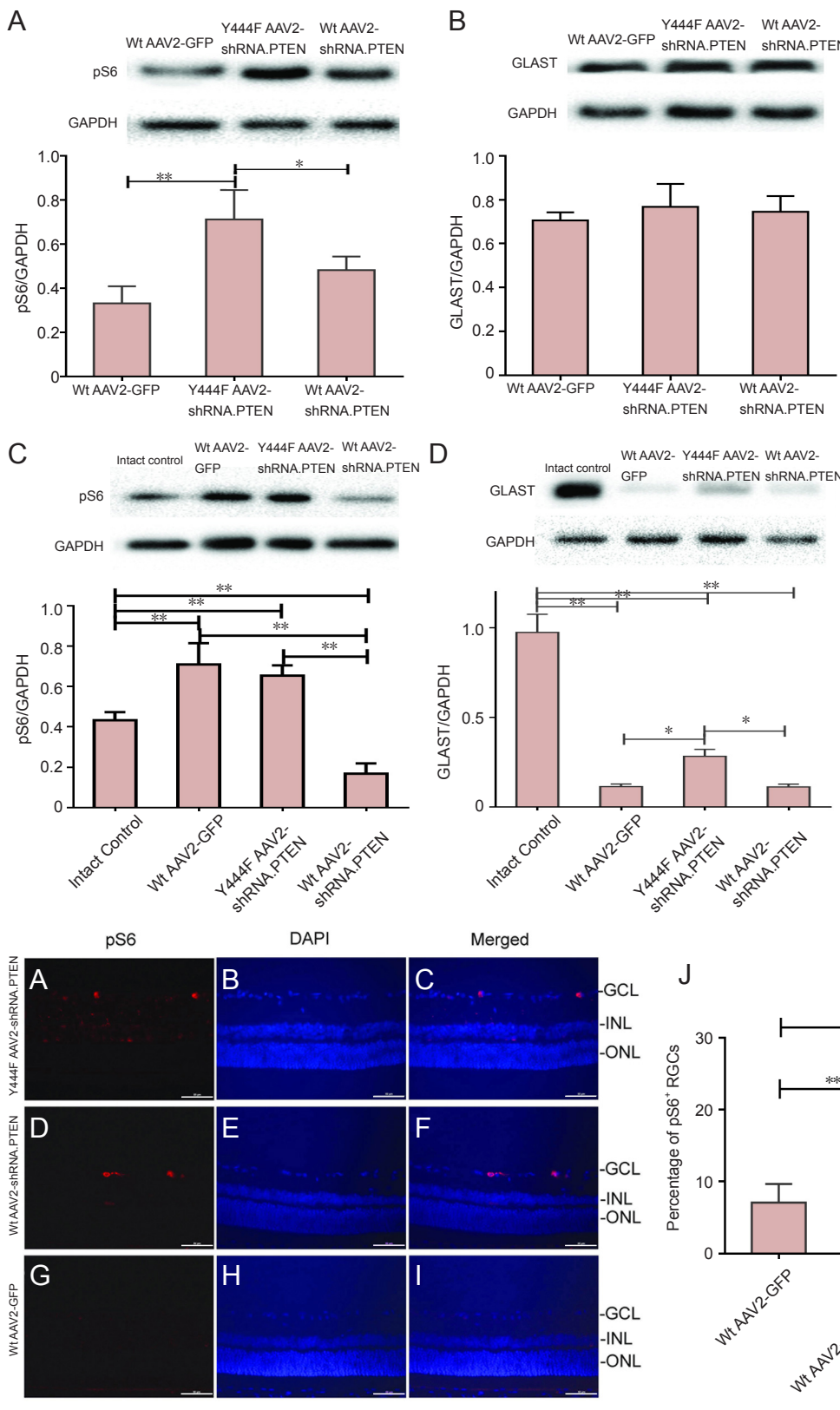
The PI3K/AKT/mTOR signaling pathway has been implicated in neuronal survival and neurite outgrowth (Christie et al., 2010; Sun et al., 2011; Guo et al., 2016). mTOR, downregulated during the development of the central nervous system and further reduced after optic nerve injury (Liu et al., 2010; Park et al., 2010), plays a critical role in modulating protein synthesis, and in axonal growth in development and in response to injury (Ma and Blenis, 2009; Lu et al., 2014). Inactivating PTEN might activate Akt and mTOR and enhance neuronal survival and axonal regeneration in optic neuropathy (Park et al., 2008; Leibinger et al., 2016). Recent studies indicate that mTOR complex-1 is necessary, while mTOR complex-2 and

GSK3b are inhibitory, for AKT3-induced axonal regeneration in the central nervous system (Miao et al., 2016). In the current study, we found that Y-to-F mutated AAV2 transduced RGCs and Müller cells more efficiently than Wt AAV2. pS6, the most widely used biochemical marker for mTOR complex-1 activity, was upregulated in both the ganglion cell layer and the inner nuclear layer of retinas infected with Y444F AAV2-shRNA.PTEN, compared with retinas infected with Wt AAV2-shRNA.PTEN, indicating that Y444F AAV2-shRNA.PTEN enhances mTOR complex-1 activity in both RGCs and Müller cells.

Another key finding of our study is that Y444F AAV2-shRNA.PTEN increased the expression of GLAST after optic nerve axotomy. Müller cells can survive under neurodegenerative conditions, and can be activated by nearly all pathogenic stimuli. Reactive Müller cells can support the survival of photoreceptors and neurons (Bringmann et al., 2009), and are considered an ideal target for viral gene therapy for neuroprotection (Bringmann et al., 2006). Expressed in Müller cells, GLAST is a major glutamate transporter within the retina, removing approximately 50% of extracellular glutamate to prevent neurotoxicity (Sarthy et al., 2005). Previous and more recent studies have shown that optic nerve crush leads to an increase in retinal extracellular glutamate to neurotoxic levels (Vorwerk et al., 2004; Nishikawa et al., 2016). The upregulation of GLAST is an anti-apoptotic response in the adult central nervous system (Koeberle and Bähr, 2008). Indeed, we observed high levels of GLAST expression 6 weeks after optic nerve axotomy in the Y444F AAV2-shRNA.PTEN group compared with the Wt AAV2-shRNA.PTEN or Wt AAV2-GFP group. Therefore, the higher GLAST expression in the transduced Müller cells might also contribute to the enhanced RGC survival. The mechanisms underlying this protective effect are unclear. However, GLAST activity might trigger  $Ca^{2+}$  influx, increase mTOR activity and promote AP-1 binding to DNA (María López-Colomé et al., 2012), in addition to preventing excitotoxicity (Izumi et al., 2002).

Here, we found that pre-administration of Y444F AAV2-shRNA.PTEN enhanced RGC survival 6 weeks after optic nerve axotomy compared with Wt AAV2-shRNA.PTEN. The survival of RGCs is a prerequisite for axonal regeneration (Morgan-Warren et al., 2013). We observed much stronger axonal regeneration in Y444F AAV2-shRNA.PTEN-injected rats, with some regenerating axons regrowing towards the optic tract. In contrast, no regenerating axons were able to reach the optic chiasm in Wt AAV2-shRNA.PTEN-injected rats. This dissimilarity might be caused by differences in mTOR complex-1 activation and GLAST expression in the transduced RGCs and Müller cells. Given that axonal regeneration induced by Y444F AAV2-shRNA.PTEN is similar to that caused by PTEN deletion (de Lima et al., 2012), it is possible that other factors also contribute to RGC survival and axonal regeneration, such as endogenous CNTF, which might be continually released by the AAV2-transduced and activated Müller glia.

We further found that RGC survival and axonal regeneration after post-axotomy injection of Y444F AAV2-shRNA.PTEN were less significant compared with pre-axotomy injection. In adult rats, RGCs start to die within 5 to 6 days of intraorbital optic nerve injury, with less than 10% surviving



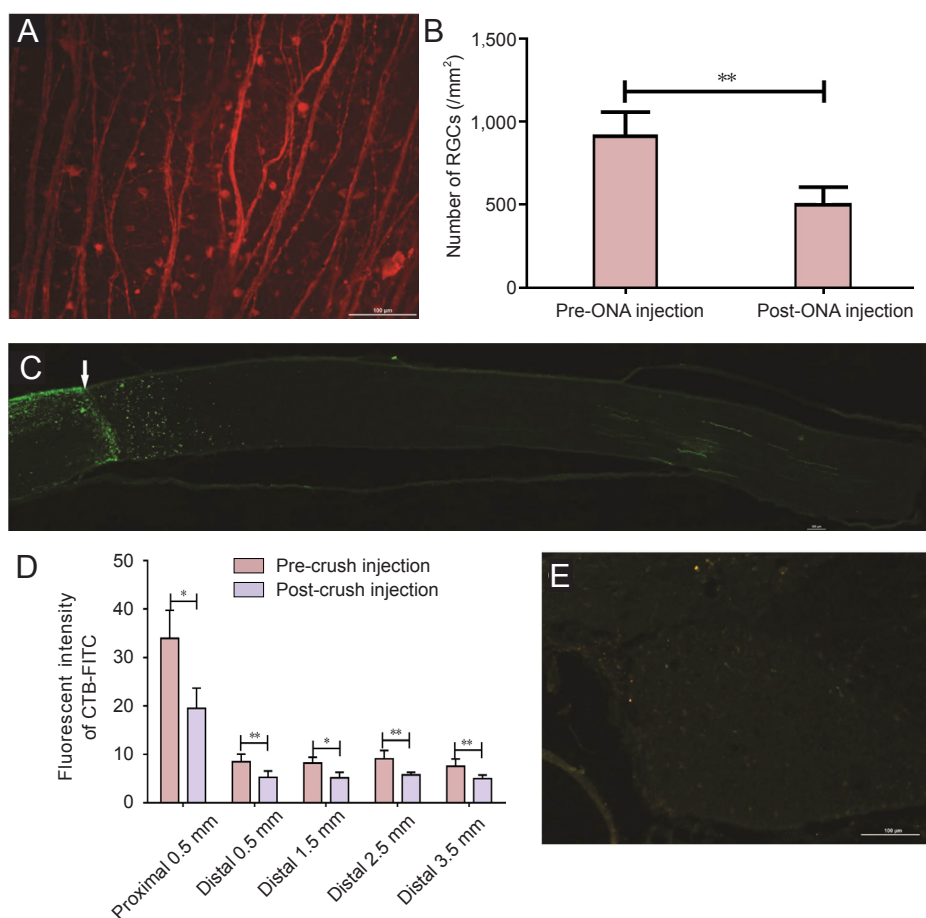


**Figure 10 RGC survival and axonal regeneration 6 weeks after post-axotomy injection of Y444F AAV2-shRNA.PTEN.**

(A, B) The number of surviving RGCs (TUJ1-immunolabeled) was significant lower in rats given post-axotomy injection of Y444F AAV2-shRNA.PTEN compared with pre-axotomy injection of the vector. (C, D) Post-axotomy injection of Y444F AAV2-shRNA.PTEN resulted in less axonal regeneration at every analyzed region of the optic nerve compared with pre-axotomy injection. (E) CTB-FITC-labeled nerve fibers were found in one of five optic chiasmata. Data are expressed as the mean  $\pm$  SD. \* $P < 0.05$ , \*\* $P < 0.01$  (Student's *t*-test). Scale bars: 100  $\mu$ m. Arrow: axotomy site. RGCs: Retinal ganglion cells; CTB-FITC: cholera toxin  $\beta$  subunit conjugated to fluorescein isothiocyanate; AAV2: adeno-associated virus 2; PTEN: phosphatase and tensin homolog; shRNA: short hairpin RNA.

by 14 days (Berkelaar et al., 1994), which is when transgene expression commences when the AAV2 vector is injected at the time of injury. Despite the rapid cell loss after optic nerve axotomy, Y444F AAV2-shRNA.PTEN injected immediately after optic nerve axotomy still rescued a considerable amount of RGCs (~19%) at 6 weeks after optic nerve axotomy. It also induced axons to regenerate up to near the optic chiasm, indicating its potential for clinical treatment.

In summary, our findings show that Y444F AAV2 is a promising vector for gene therapy for traumatic optic neuropathy. Y444F AAV2-mediated PTEN knockdown was able to activate mTOR complex-1 and induce long-distance axonal regeneration in wildtype animals, suggesting that it is a promising translatable treatment for traumatic optic neuropathy. In view of the complexity of the cell and molecular mechanisms underlying axonal regeneration, future studies will focus on using Y444F AAV2 to modulate mTOR complex-1 as well as other critical targets to achieve robust axonal regeneration for functional visual recovery.

**Author contributions:** ZRH contributed to the conception, design, execution and analysis of all experiments and paper writing. HYC, ZZH, and PX were in charge of experimental execution. QHL was responsible for the conception and design of the experiments, paper writing, and generated the AAV vectors. All authors approved the final version of the paper.

**Conflicts of interest:** None declared.

**Financial support:** This study was supported by the Research Foundation of Jiangsu Provincial Commission of Health and Family Planning of China, No. H201653, and the Research Foundation of Changshu Science and Technology Bureau of China, No. CS201616. None of the funding bodies play any role in the study other than to provide funding.

**Research ethics:** The study protocol was approved by the Institutional

Animal Care and Use Committee of Nanjing Medical University of China (approval No. 2015-0076).

**Data sharing statement:** Datasets analyzed during the current study are available from the corresponding author on reasonable request.

**Plagiarism check:** Checked twice by iThenticate.

**Peer review:** Externally peer reviewed.

**Open access statement:** This is an open access article distributed under the terms of the Creative Commons Attribution-NonCommercial-ShareAlike 3.0 License, which allows others to remix, tweak, and build upon the work non-commercially, as long as the author is credited and the new creations are licensed under identical terms.

## References

- Auricchio A, Kobinger G, Anand V, Hildinger M, O'Connor E, Maguire AM, Wilson JM, Bennett J (2001) Exchange of surface proteins impacts on viral vector cellular specificity and transduction characteristics: the retina as a model. *Hum Mol Genet* 10:3075-3081.
- Benowitz LI, He Z, Goldberg JL (2017) Reaching the brain: Advances in optic nerve regeneration. *Exp Neurol* 287:365-373.
- Berkelaar M, Clarke DB, Wang YC, Bray GM, Aguayo AJ (1994) Axotomy results in delayed death and apoptosis of retinal ganglion cells in adult rats. *J Neurosci* 14:4368-4374.
- Boye SE, Alexander JJ, Witherspoon CD, Boye SL, Peterson JJ, Clark ME, Sandefer KJ, Girkin CA, Hauswirth WW, Gamlin PD (2016) Highly efficient delivery of adeno-associated viral vectors to the primate retina. *Hum Gene Ther* 27:580-597.
- Bringmann A, Pannicke T, Grosche J, Francke M, Wiedemann P, Skatchkov SN, Osborne NN, Reichenbach A (2006) Müller cells in the healthy and diseased retina. *Prog Retin Eye Res* 25:397-424.
- Bringmann A, Iandiev I, Pannicke T, Wurm A, Hollborn M, Wiedemann P, Osborne NN, Reichenbach A (2009) Cellular signaling and factors involved in Müller cell gliosis: neuroprotective and detrimental effects. *Prog Retin Eye Res* 28:423-451.
- Cen LP, Liang JJ, Chen JH, Harvey AR, Ng TK, Zhang M, Pang CP, Cui Q, Fan YM (2017) AAV-mediated transfer of RhoA shRNA and CNTF promotes retinal ganglion cell survival and axon regeneration. *Neuroscience* 343:472-482.

- Christie KJ, Webber CA, Martinez JA, Singh B, Zochodne DW (2010) PTEN inhibition to facilitate intrinsic regenerative outgrowth of adult peripheral axons. *J Neurosci* 30:9306-9315.
- de Lima S, Koriyama Y, Kurimoto T, Oliveira JT, Yin Y, Li Y, Gilbert HY, Fagioli M, Martinez AM, Benowitz L (2012) Full-length axon regeneration in the adult mouse optic nerve and partial recovery of simple visual behaviors. *Proc Natl Acad Sci U S A* 109:9149-9154.
- Ding W, Zhang LN, Yeaman C, Engelhardt JF (2006) rAAV2 traffics through both the late and the recycling endosomes in a dose-dependent fashion. *Mol Ther* 13:671-682.
- Fischer D, Leibinger M (2012) Promoting optic nerve regeneration. *Prog Retin Eye Res* 31:688-701.
- Goldberg JL (2004) Intrinsic neuronal regulation of axon and dendrite growth. *Curr Opin Neurobiol* 14:551-557.
- Guo X, Snider WD, Chen B (2016) GSK3beta regulates AKT-induced central nervous system axon regeneration via an eIF2Bepsilon-dependent, mTORC1-independent pathway. *Elife* 5:e11903.
- Guzman-Aranguez A, Loma P, Pintor J (2013) Small-interfering RNAs (siRNAs) as a promising tool for ocular therapy. *Br J Pharmacol* 170:730-747.
- Harvey AR, Hu Y, Leaver SG, Mellough CB, Park K, Verhaagen J, Plant GW, Cui Q (2006) Gene therapy and transplantation in CNS repair: the visual system. *Prog Retin Eye Res* 25:449-489.
- Hellström M, Harvey AR (2011) Retinal ganglion cell gene therapy and visual system repair. *Curr Gene Ther* 11:116-131.
- Hellström M, Pollett MA, Harvey AR (2011) Post-injury delivery of rAAV2-CNTF combined with short-term pharmacotherapy is neuroprotective and promotes extensive axonal regeneration after optic nerve trauma. *J Neurotrauma* 28:2475-2483.
- Hellstrom M, Ruitenber MJ, Pollett MA, Ehlert EM, Twisk J, Verhaagen J, Harvey AR (2009) Cellular tropism and transduction properties of seven adeno-associated viral vector serotypes in adult retina after intravitreal injection. *Gene Ther* 16:521-532.
- Izumi Y, Shimamoto K, Benz AM, Hammerman SB, Olney JW, Zorumski CF (2002) Glutamate transporters and retinal excitotoxicity. *Glia* 39:58-68.
- Koch JC, Barski E, Lingor P, Bähr M, Michel U (2011a) Plasmids containing NRSE/RE1 sites enhance neurite outgrowth of retinal ganglion cells via sequestration of REST independent of NRSE dsRNA expression. *FEBS J* 278:3472-3483.
- Koch JC, Knöferle J, Tönges L, Michel U, Bähr M, Lingor P (2011b) Imaging of rat optic nerve axons in vivo. *Nat Protocols* 6:1887-1896.
- Koch JC, Tonges L, Barski E, Michel U, Bähr M, Lingor P (2014) ROCK2 is a major regulator of axonal degeneration, neuronal death and axonal regeneration in the CNS. *Cell Death Dis* 5:e1225.
- Koeberle PD, Bähr M (2008) The upregulation of GLAST-1 is an indirect antiapoptotic mechanism of GDNF and neurturin in the adult CNS. *Cell Death Differ* 15:471-483.
- Leibinger M, Andreadaki A, Gobrecht P, Levin E, Diekmann H, Fischer D (2016) Boosting Central Nervous System Axon Regeneration by Circumventing Limitations of Natural Cytokine Signaling. *Mol Ther* 24:1712-1725.
- Lewandowski G, Steward O (2014) AAVshRNA-mediated suppression of PTEN in adult rats in combination with salmon fibrin administration enables regenerative growth of corticospinal axons and enhances recovery of voluntary motor function after cervical spinal cord injury. *J Neurosci* 34:9951-9962.
- Liang FQ, Surace E, Dejneka NS, Maguire AM, Bennett J (2003) Müller cell transduction by AAV2 in normal and degenerative retinas. *Adv Exp Med Biol* 533:439-445.
- Liu K, Lu Y, Lee JK, Samara R, Willenberg R, Sears-Kraxberger I, Tedeschi A, Park KK, Jin D, Cai B, Xu B, Connolly L, Steward O, Zheng B, He Z (2010) PTEN deletion enhances the regenerative ability of adult corticospinal neurons. *Nat Neurosci* 13:1075-1081.
- Lu Y, Belin S, He Z (2014) Signaling regulations of neuronal regenerative ability. *Curr Opin Neurobiol* 27:135-142.
- Ma XM, Blenis J (2009) Molecular mechanisms of mTOR-mediated translational control. *Nat Rev Mol Cell Biol* 10:307-318.
- María López-Colomé A, Martínez-Lozada Z, Guillem AM, López E, Ortega A (2012) Glutamate transporter-dependent mTOR phosphorylation in Müller glia cells. *ASN Neuro* 4:e00095.
- Miao L, Yang L, Huang H, Liang F, Ling C, Hu Y (2016) mTORC1 is necessary but mTORC2 and GSK3beta are inhibitory for AKT3-induced axon regeneration in the central nervous system. *Elife* 5:e14908.
- Moore DL, Goldberg JL (2010) Four steps to optic nerve regeneration. *J Neuroophthalmol* 30:347-360.
- Morgan-Warren PJ, Berry M, Ahmed Z, Scott RA, Logan A (2013) Exploiting mTOR signaling: a novel translatable treatment strategy for traumatic optic neuropathy? *Invest Ophthalmol Vis Sci* 54:6903-6916.
- Newman E, Reichenbach A (1996) The Muller cell: a functional element of the retina. *Trends Neurosci* 19:307-312.
- Nishikawa Y, Oku H, Morishita S, Horie T, Kida T, Mimura M, Fukumoto M, Kojima S, Ikeda T (2016) Negative impact of AQP-4 channel inhibition on survival of retinal ganglion cells and glutamate metabolism after crushing optic nerve. *Exp Eye Res* 146:118-127.
- Park KK, Liu K, Hu Y, Kanter JL, He Z (2010) PTEN/mTOR and axon regeneration. *Exp Neurol* 223:45-50.
- Park KK, Liu K, Hu Y, Smith PD, Wang C, Cai B, Xu B, Connolly L, Kramvis I, Sahin M, He Z (2008) Promoting axon regeneration in the adult CNS by modulation of the PTEN/mTOR pathway. *Science* 322:963-966.
- Petrs-Silva H, Dinculescu A, Li Q, Min SH, Chiodo V, Pang JJ, Zhong L, Zolotukhin S, Srivastava A, Lewin AS, Hauswirth WW (2009) High-efficiency transduction of the mouse retina by tyrosine-mutant AAV serotype vectors. *Mol Ther* 17:463-471.
- Petrs-Silva H, Dinculescu A, Li Q, Deng WT, Pang JJ, Min SH, Chiodo V, Neeley AW, Govindasamy L, Bennett A, Agbandje-McKenna M, Zhong L, Li B, Jayandharan GR, Srivastava A, Lewin AS, Hauswirth WW (2011) Novel properties of tyrosine-mutant AAV2 vectors in the mouse retina. *Mol Ther* 19:293-301.
- Sarthy VP, Pignataro L, Pannicke T, Weick M, Reichenbach A, Harada T, Tanaka K, Marc R (2005) Glutamate transport by retinal Muller cells in glutamate/aspartate transporter-knockout mice. *Glia* 49:184-196.
- Sun F, Park KK, Belin S, Wang D, Lu T, Chen G, Zhang K, Yeung C, Feng G, Yankner BA, He Z (2011) Sustained axon regeneration induced by co-deletion of PTEN and SOCS3. *Nature* 480:372-375.
- Tshilenge KT, Ameline B, Weber M, Mendes-Madeira A, Nedellec S, Biget M, Provost N, Libeau L, Blouin V, Deschamps JY, Le Meur G, Colle MA, Moullier P, Pichard V, Rolling F (2016) Vitrectomy before intravitreal injection of AAV2/2 vector promotes efficient transduction of retinal ganglion cells in dogs and nonhuman primates. *Hum Gene Ther Methods* 27:122-134.
- Vorwerk CK, Zurakowski D, McDermott LM, Mawrin C, Dreyer EB (2004) Effects of axonal injury on ganglion cell survival and glutamate homeostasis. *Brain Res Bull* 62:485-490.
- Woodard KT, Liang KJ, Bennett WC, Samulski RJ (2016) Heparan sulfate binding promotes accumulation of intravitreally delivered adeno-associated viral vectors at the retina for enhanced transduction but weakly influences tropism. *J Virol* 90:9878-9888.
- Xie Q, Bu W, Bhatia S, Hare J, Somasundaram T, Azzi A, Chapman MS (2002) The atomic structure of adeno-associated virus (AAV-2), a vector for human gene therapy. *Proc Natl Acad Sci U S A* 99:10405-10410.
- Yang P, Yang Z (2012) Enhancing intrinsic growth capacity promotes adult CNS regeneration. *J Neurosci* 31:1-6.
- Zaiss AK, Foley EM, Lawrence R, Schneider LS, Hoveida H, Secret P, Catapang AB, Yamaguchi Y, Alemany R, Shayakhmetov DM, Esko JD, Herschman HR (2015) Hepatocyte heparan sulfate is required for adeno-associated virus 2 but dispensable for adenovirus 5 liver transduction in vivo. *J Virol* 90:412-420.
- Zhong L, Li B, Jayandharan G, Mah CS, Govindasamy L, Agbandje-McKenna M, Herzog RW, Weigel-Van Aken KA, Hobbs JA, Zolotukhin S, Muzyczka N, Srivastava A (2008a) Tyrosine-phosphorylation of AAV2 vectors and its consequences on viral intracellular trafficking and transgene expression. *Virology* 381:194-202.
- Zhong L, Li B, Mah CS, Govindasamy L, Agbandje-McKenna M, Cooper M, Herzog RW, Zolotukhin I, Warrington KH Jr, Weigel-Van Aken KA, Hobbs JA, Zolotukhin S, Muzyczka N, Srivastava A (2008b) Next generation of adeno-associated virus 2 vectors: point mutations in tyrosines lead to high-efficiency transduction at lower doses. *Proc Natl Acad Sci U S A* 105:7827-7832.
- Zolotukhin S, Byrne BJ, Mason E, Zolotukhin I, Potter M, Chesnut K, Summerford C, Samulski RJ, Muzyczka N (1999) Recombinant adeno-associated virus purification using novel methods improves infectious titer and yield. *Gene Ther* 6:973-985.

(Copolyedited by Patel B, Wysong S, Yu J, Li CH, Qiu Y, Song LP, Zhao M)